ISSN 1069-3513, Izvestiya, Physics of the Solid Earth, 2021, Vol. 57, No. 2, pp. 279–288. © Pleiades Publishing, Ltd., 2021.
Russian Text © The Author(s), 2021, published in Fizika Zemli, 2021, No. 2, pp. 153–163.

The Relationship between Multifractal and Entropy Properties of Seismic Noise in Kamchatka and Irregularity of the Earth's Rotation

A. A. Lyubushin[a], *, G. N. Kopylova[b], **, and Yu. K. Serafimova[b], ***

[a] *Schmidt Institute of Physics of the Earth, Russian Academy of Sciences, Moscow, 123242 Russia*

[b] *Kamchatka Branch, Federal Research Center "Geophysical Survey of the Russian Academy of Sciences," Petropavlovsk-Kamchatskii, 683006 Russia*

**e-mail: lyubushin@yandex.ru*

***e-mail: gala@emsd.ru*

****e-mail: yulka@emsd.ru*

Received February 11, 2020; revised August 8, 2020; accepted August 8, 2020

Abstract—The connection between the properties of seismic noise continuously recorded by the network of 21 broadband seismic stations in Kamchatka during nine years of observations (2011–2019) and the nonuniform rotation of the Earth is studied. The daily time series of median values calculated over all network stations are analyzed for three noise parameters: multifractal singularity spectrum support width, generalized Hurst exponent, and minimum entropy of the distribution of the squared orthogonal wavelet coefficients. For identifying the common components in the variations of these parameters, their adaptive first principal component was calculated in a half-year moving window. The quadratic coherence spectrum between the first principal component of seismic noise characteristics and the time series of the length of the day was calculated in a 182-day moving time window. The time–frequency diagram of the coherence spectrum characterized by a sequence of coherence bursts concentrated in a narrow frequency band with periods from 11 to 14 days is analyzed. The time delays between the coherence bursts and the release of seismic energy in Kamchatka are estimated in a 5-year moving time window.

Keywords: seismic noise, multifractals, entropy, principal component analysis, coherence, irregularity of the Earth's rotation

DOI: 10.1134/S106935132102004X

INTRODUCTION

The nonuniform rotation of the Earth has historically attracted interest of geophysicists. The explanation of this effect mainly relies on the estimates of the influence of atmospheric processes (Levitskii et al., 1995; Sidorenkov, 2002; Zotov et al., 2017). At the same time, many researchers have repeatedly pointed out the connection between the irregular rotation of the Earth and seismicity (Guberman, 1976; Sasorova and Levin, 2017; Shanker et al., 2001; Levin et al., 2017). The main attention in this context was focused on the probable triggering mechanism of the influence of variations in the Earth's rotation on seismic process (Bendick and Bilham, 2017). We note that this interpretation raises a natural question about the impact of the atmospheric processes including climate variations through the nonuniform rotation of the Earth.

In this paper, we analyze the relationship between seismic noise on the Kamchatka Peninsula—one of the world's most seismically active regions,—and the length of day (LOD) parameter whose time series characterize the irregularity in the rotation velocity of the Earth. The relationship between the characteristics of the global seismic noise and LOD time series was previously studied in (Lyubushin, 2020a; 2020b)

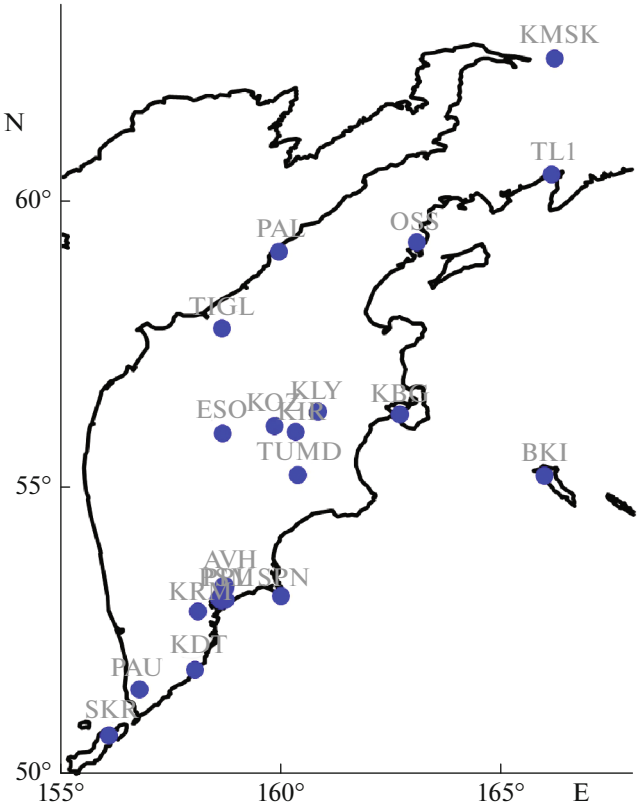

Fig. 1. Circles show positions of 21 seismic stations in Kamchatka. Station codes are indicated near each station.

where it was shown that the middle of 2003 was a breaking point in the trends and correlations of the characteristics of global seismic noise. Since 2003, the behavior of global seismic noise has characteristic trends of the regions with the increasing seismic hazard. We note that after the Sumatra mega-earthquake of December 26, 2004, $M = 9$, the number of strongest earthquakes all over the world sharply increased. The novelty of this study is that the previously developed approach is used to analyze the data for Kamchatka.

Seismic noise is considered as a manifestation of the internal life of the Earth and as an important "communication link" that allows for the study of the processes in the lithosphere including those before the strong earthquakes (Lyubushin, 2007; 2009; 2014; Sobolev, 2014; Lyubushin, 2018). The prognostic characteristics of seismic noise in Kamchatka were previously analyzed in (Kasimova et al., 2018; Lyubushin et al., 2015).

INITIAL DATA

Seismicity in the territory of the Kamchatka Krai is monitored by a network of digital broadband seismic stations whose data are transmitted in real time to the Information Processing Center of the Kamchatka Branch of the Geophysical Survey of Russian Academy of Sciences (KB GS RAS) via satellites and other communication channels (Chebrov, 2013; Chebrov et al., 2013). In this work we analyze the data on the vertical (BHZ) component of ground motion recorded with a sampling frequency of 100 Hz by 21 broadband seismic stations GS RAS from January 1, 2011 to December 31, 2019 in the territory of the Kamchatka Krai and Paramushir Island, the Kuriles (Fig. 1).

For constructing 1-min time series of low-frequency noise recorded by each station, we calculated the averages of the initial records in the successive time windows of 6000 counts (time points). The resulting 1-min time series for the 21 stations are stored in the continuously updated database on the server of the KB GS RAS accessible via the local network. The measurements are conducted by CMG-6TD, CMG-3TV, and KS2000 type seismic sensors described in (Kasimova et al., 2018; Lyubushin et al., 2015).

An important debatable question in applying the discussed technique for studying the characteristics of the low-frequency ambient seismic noise is that, formally, the frequency range of the signals recorded by seismic sensors does not include periods from 2 to ~1000 min which are, in fact, analyzed when we pass to 1-min data on time intervals with a length of one day. This raises a natural question of whether the transition to this low-frequency region of the records of seismic signal is legitimate.

Here, we rely on the assumption that instrumental limitations on low frequency of the signal are only provided for the correct display of ground motions from separate earthquakes and for quantitative determination of their parameters. It should be noted that the designers of broadband seismic instruments did not envisage probable use of the continuously logged seismic records in a wider frequency range exceeding the upper frequency limit of the signals from earthquakes. It was also not expected that seismic sensors could be used as a conventional tiltmeter, i.e. that they detect ground motions in the tidal frequency band. We believe that in the problems of geophysical monitoring, there is a fundamental possibility of a wider scope for applying the broadband seismic instruments which transcends the formal limitations on working frequencies traditionally used in the studies of individual earthquakes.

This issue has been already discussed in our previous works (Kasimova et al., 2018; Lyubushin et al., 2015). In particular, power spectra estimates were presented for seismic records resampled to a time step of 1 h, i.e., with a substantially deeper averaging than used in the analysis in this paper. In the cited works it was shown that these spectra contain standard tidal harmonics which means that broadband seismometers can, in fact, operate as tiltmeters in the frequency range extending far beyond their formal limits.

Revisiting this issue in this paper, we estimate power spectra of the records after the transition to

1-min sampling interval in the intermediate frequency between seismological and tiltmeter ones, which covers periods from 2 to 1000 min. It is known that this frequency range contains spectral peaks corresponding to the free oscillations of the Earth continuously excited by the earthquakes (Milyukov et al., 2015). But are these peaks present in the spectrum of seismic records after the transition to a sampling interval of 1 min? Figure 2 shows power spectra estimates for eight seismic stations. It can be seen that almost all spectra contain a set of monochromatic harmonics corresponding to different modes of the free background oscillations of the Earth (FOE) excited by seismic events, in particular, the lowest-frequency FOE harmonic with a period close to 60 min.

Thus, we believe that the transition to the low-frequency part of the spectrum by averaging the seismic records and reducing them to 1-min sampling interval does not completely destroy substantive information contained in the records. Moreover, it is the transition to the low-frequency part of the spectrum that allows bypassing most of the anthropogenic impacts and to studying the prognostic characteristics of the free background oscillations of the Earth. This transition has been on many occasions used in the previous works (Lyubushin, 2007; 2009; 2014; 2010a; 2010b; 2012; 2013; 2014; 2018; 2020a; 2020b) in the analysis of the continuous records of seismic noise from broadband networks.

CHARACTERISTICS OF SEISMIC NOISE EMPLOYED IN THE STUDY

Below we describe three dimensionless characteristics of seismic noise which were calculated for vertical ground motions after the transition to a sampling interval of 1 min for each station in the successive time windows with a length of one day (1440 one-minute values or data points). Before calculating these characteristics, seismic noise waveforms in each time window were detrended using the 8th order orthogonal polynomial. Detrending suppresses the effects of tidal and thermal deformations of the Earth's crust in the variations in seismic noise and is a mandatory procedure in the studies of its statistical characteristics. Using the orthogonal polynomial ensures stability of the estimate of the trend values at sampling points. The polynomial order (8) was selected based on the results of numerical calculations as the smallest order guaranteeing the removal of diurnal and semidiurnal variations on daily intervals.

Multifractal Parameters $\Delta\alpha$ and α^*

We consider a random oscillation $x(t)$ on time interval $[t - \delta/2, t + \delta/2]$ with length δ centered at time point t. Let us analyze the range of the random oscillation on this interval, i.e., the difference between the maximum and minimum values (peak-to-peak amplitude):

$$\mu(t,\delta) = \max_{t-\delta/2 \le s \le t+\delta/2} x(s) - \min_{t-\delta/2 \le s \le t+\delta/2} x(s). \quad (1)$$

If $\delta \to 0$, then $\mu(t,\delta)$ also tends to zero but what is important here is the rate of this decay. If the decay rate is determined by the law $\delta^{h(t)}$: $\mu(t,\delta) \sim \delta^{h(t)}$ at $\delta \to 0$, or if the limit $h(t) = \lim_{\delta\to 0} \dfrac{\log(\mu(t,\delta))}{\log(\delta)}$ exists, then quantity $h(t)$ is called the Hölder–Lipschitz exponent. If the $h(t)$ value does not depend on time t: $h(t) = \text{const} = H$, then random oscillation $x(t)$ is called monofractal and H is called the Hurst exponent. If the Hölder–Lipschitz exponents differ substantially for different moments of time, then the random oscillation is called a multifractal and for this oscillation the notion of singularity spectrum can be defined (Feder, 1988). For doing this, we mentally select the set $C(\alpha)$ of the moments of time having the same value of the Hölder–Lipschitz exponent $h(t) = \alpha$. Sets $C(\alpha)$ do not exist for every α value (to exist means to contain some elements and to be not the empty set). That is, there are some minimum $\alpha_{\min}$ and maximum $\alpha_{\max}$ such that only for $\alpha_{\min} < \alpha < \alpha_{\max}$ are the sets $C(\alpha)$ nonempty. The multifractal singularity spectrum $F(\alpha)$ is a fractal dimension of set of points $C(\alpha)$ of. Parameter $\Delta\alpha = \alpha_{\max} - \alpha_{\min}$ which is called the singularity spectrum support width is perhaps a most important multifractal characteristic. Yet another interesting pertinent parameter is the argument α^* that maximizes the singularity spectrum $F(\alpha^*) = \max_{\alpha_{\max} \le \alpha \le \alpha_{\min}} F(\alpha)$. This parameter is called the generalized Hurst exponent. The maximum of the singularity spectrum cannot be greater than unity which is the dimension of the enclosing set or time axis, $0 < F(\alpha^*) \le 1$, typically $F(\alpha^*) = 1$. We note that for a monofractal signal, $\Delta\alpha = 0$, $\alpha^* = H$. By definition, $\Delta\alpha$ is the measure of diversity of random behavior of a signal, which reflects the number of the Hölder–Lipschitz exponents. In a simple monofractal random signal there is only one Hölder–Lipschitz exponent, which is the very same the Hurst exponent. Therefore, a decrease in $\Delta\alpha$ is the sign indicating that certain degrees of freedom of the system generating the studied signal are suppressed and also the sign of the reduction of their number. The method used for calculating parameters $\Delta\alpha$ and $\alpha^*$is described in detail in (Lyubushin, 2007; 2009; 2010; 2014; 2018).

Minimum Normalized Entropy En of Wavelet Coefficients

Let $x(t)$ be a finite sample of some random signal, $t = 1,\ldots,N$ be the index numbering the successive sig-

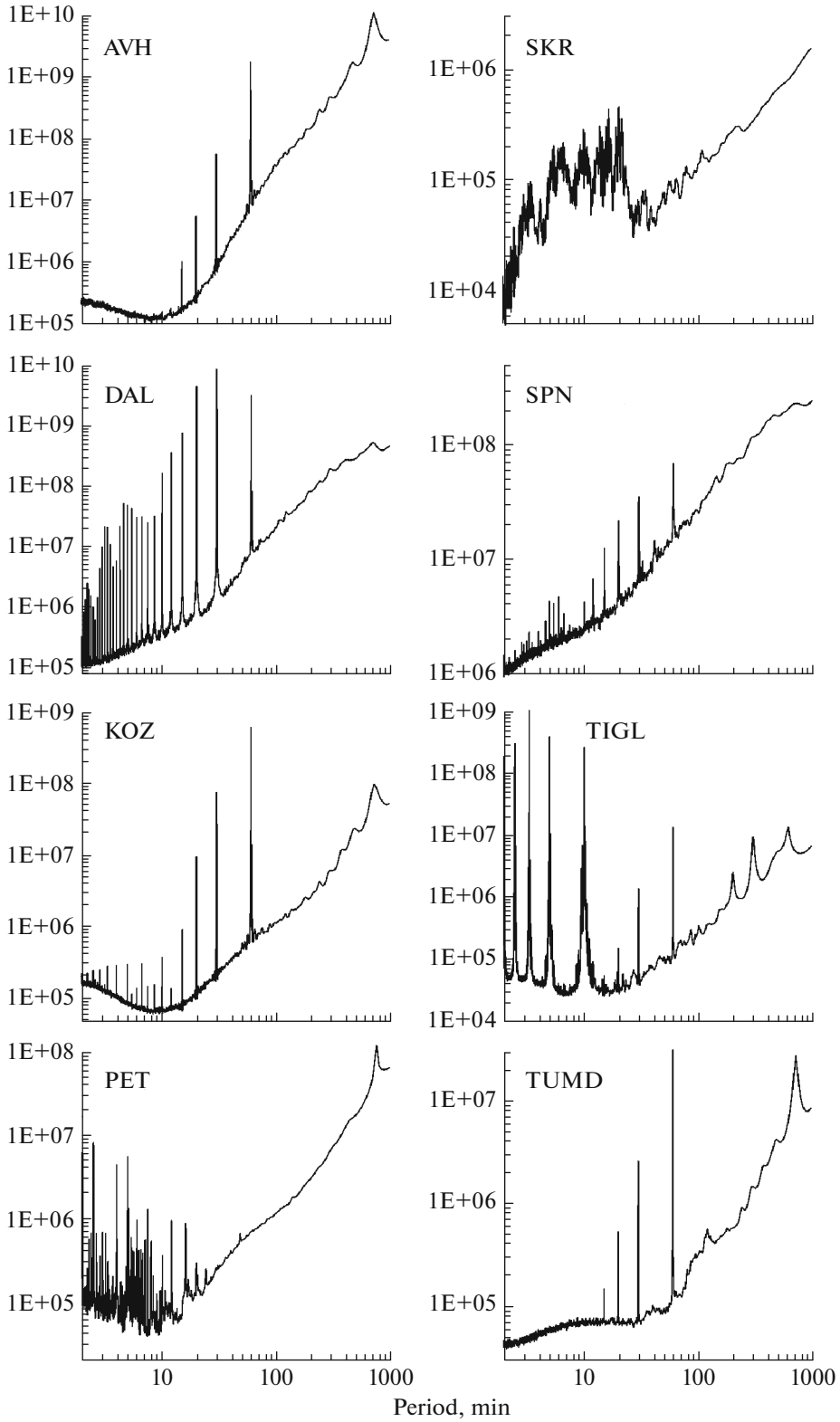

Fig. 2. Graphs of power spectra estimates of seismic records after transition to 1-min sampling for eight network stations in frequency range corresponding to periods from 2 to 1000 min.

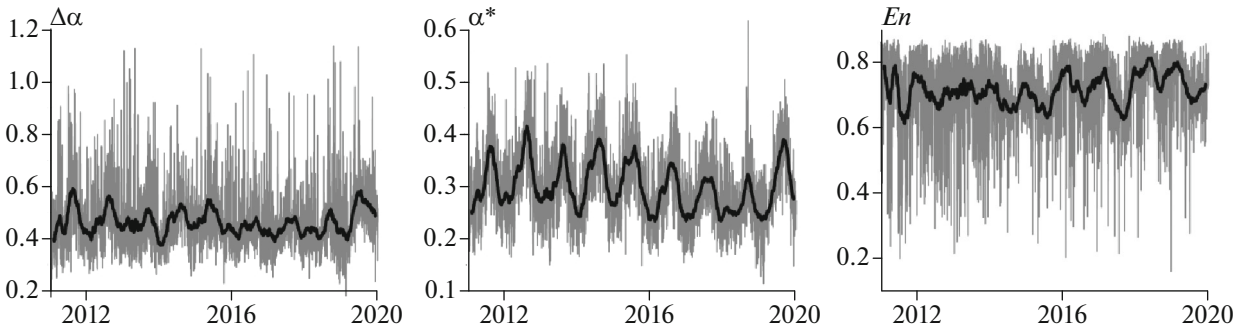

Fig. 3. Graphs of daily median values for three dimensionless parameters of seismic noise in Kamchatka. Heavy lines show moving averages in 57-day window.

nal values (discrete time). We define the normalized entropy of the final sample by the following formula:

$$En = -\sum_{k=1}^{N} p_k \log(p_k)\Big/\log(N),$$
$$p_k = c_k^2\Big/\sum_{j=1}^{N} c_j^2, \quad 0 \le En \le 1. \tag{2}$$

Here c_k, $k = 1, N$ are the coefficients of the orthogonal wavelet decomposition with some basis. Below we used 17 orthogonal Daubechies wavelets: ten ordinary bases with a minimum support with one to ten vanishing moments and seven the so-called Daubechies simlets (Mallat, 1999) with four to ten vanishing moments. For each basis, we calculated the normalized entropy of the distribution of squared coefficients (2) and found the basis that provides minimum to (2). We note that due to the orthogonality of the wavelet transform, the sum of the squares of the coefficients is equal to the variance (energy) of the signal $x(t)$. Thus, the quantity (2) calculates the entropy of the energy distribution of the oscillation on different frequency and time scales.

Statistics $\Delta\alpha$, α^* and En were used in (Lyubushin, 2007; 2009; 2010; 2012; 2013; 2014a; 2014b; 2018; 2020c) for studying the synchronization characteristics of the global field of seismic noise and the prognostic characteristics of seismic noise in the Islands of Japan and in California.

For each property and for every day, we calculated the median values of the characteristics ($En, \Delta\alpha, \alpha^*$) for all operational stations. Thus, we obtained three time series with daily sampling interval for 2011–2019. The graphs are shown in Fig. 3.

ADAPTIVE PRINCIPAL COMPONENT METHOD

The time series ($En, \Delta\alpha, \alpha^*$) need to be aggregated into a single time series that bears the most generic properties of the initial set of parameters characterizing the noise. We used here a modification of the well-known principal component method (Aivazyan et al., 1989; Jolliffe, 1986) proposed in (Lyubushin, 2018). Let $P(t) = (P_1(t),\ldots,P_m(t))^T$, $t = 0,1,\ldots$ be several time series with total dimension m. In our case, $m = 3$. Let L be the number of points within the time window that moves from left to right with a minimum mutual shift of 1, which we call the adaptation window. Let s be the number of the point corresponding to the right end of the moving time window. This means that the time window contains samples with the time indices obeying the condition $s - L + 1 \le t \le s$. Let us calculate the $m \times m$ correlation matrix $\Phi(s)$ in each time window after the normalization of the time series components:

$$\Phi(s) = \left(\varphi_{ab}^{(s)}\right), \quad \varphi_{ab}^{(s)} = \sum_{t=s-L+1}^{s} q_a^{(s)}(t) q_b^{(s)}(t)\Big/L, \quad a,b = 1,\ldots,m, \tag{3}$$

where

$$q_a^{(s)}(t) = \left(P_a(t) - \overline{P}_a^{(s)}\right)\Big/\sigma_a^{(s)},$$
$$\overline{P}_a^{(s)} = \sum_{t=s-L+1}^{s} P_a(t)\Big/L,$$
$$\left(\sigma_a^{(s)}\right)^2 = \sum_{t=s-L+1}^{s} \left(P_a(t) - \overline{P}_a^{(s)}\right)^2\Big/(L-1), \quad a = 1,\ldots,m. \tag{4}$$

The first principal component $\psi^{(s)}(t)$ is calculated by the following formula:

$$\psi^{(s)}(t) = \sum_{\alpha=1}^{m} \theta_a^{(s)} q_a^{(s)}(t). \tag{5}$$

Here the m-dimensional vector $\theta^{(s)} = (\theta_1^{(s)},\ldots,\theta_m^{(s)})^T$ is the eigenvector of the correlation matrix $\Phi(s)$ corresponding to the maximum eigenvalue. Let us determine the scalar time series of the adaptive first principal component $\psi(t)$ in a moving window with a length L points by the formula

$$\psi(t) = \begin{cases} \psi^{(L-1)}(t), & 0 \le t \le (L-1) \\ \psi^{(t)}(t), & t \ge L. \end{cases} \tag{6}$$

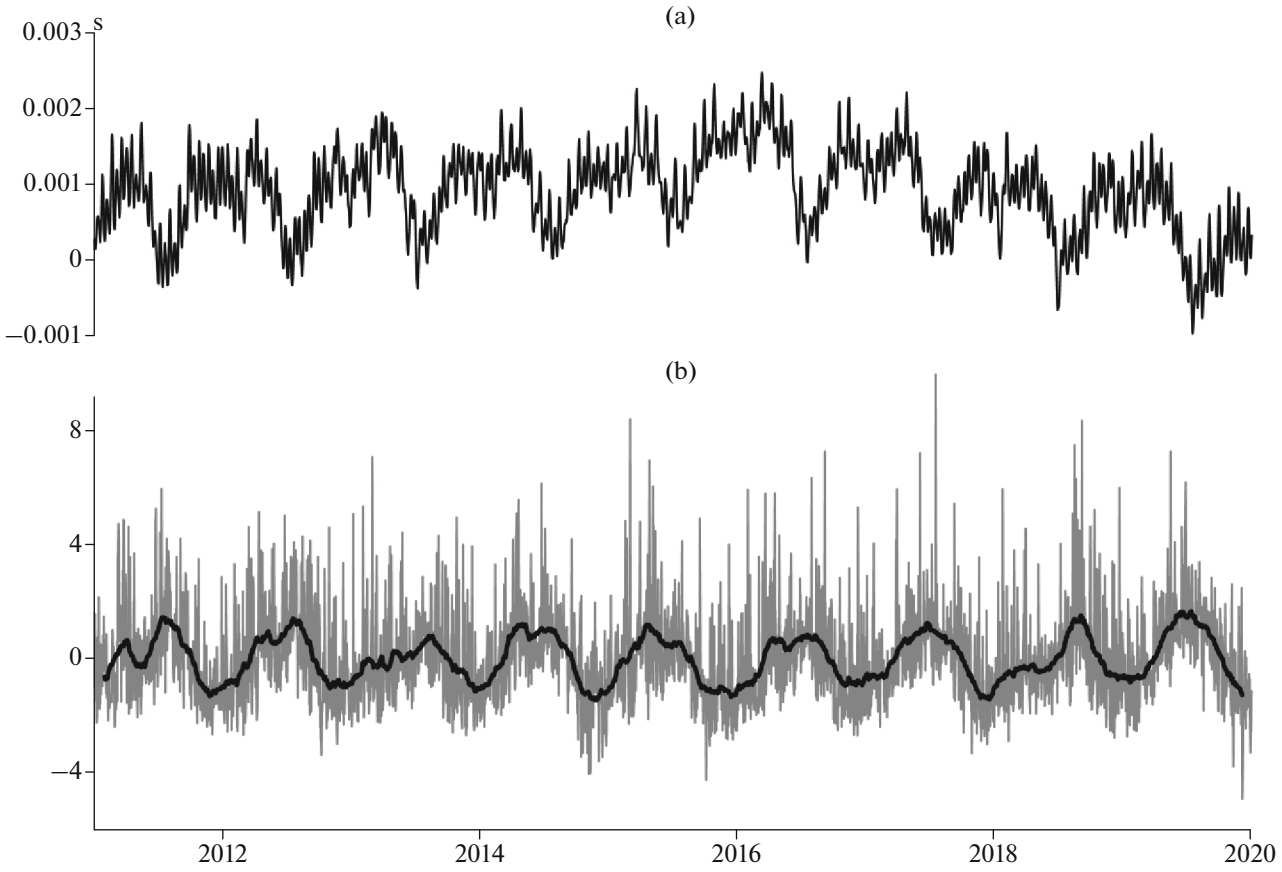

Fig. 4. (a) Length-of-day (LOD) time series; (b) first principal component for three daily median values of seismic noise in Kamchatka calculated in 182-day window. Heavy line shows moving averages in 57-day window.

The operations described by formulas (3)–(5) are carried out independently in each time window with a length of L points. Thus, within the first adaptation time window, time series $\psi(t)$ consists of the values calculated by (5), whereas for all subsequent time indices it is equal to the value of (5) corresponding to the rightmost end of the time window, i.e., beyond the first adaptation window $\psi(t)$ only depends on the past values of $P(t)$.

Figure 4 shows the graphs of the time series of LOD (length of day) characterizing the irregularity of the rotation of the Earth and the main component of daily time series of three characteristics ($En, \Delta\alpha, \alpha^*$) in the moving adaptation window with length $L = 182$ days (six months). The LOD data are taken from the International Earth rotation and Reference systems Service (IERS) database at https://hpiers.obspm.fr/iers/eop/eopc04/eopc04.62-now.

ESTIMATING THE COHERENCE SPECTRUM

For analyzing the relationship between the characteristics of seismic noise and the irregularity of the Earth's rotation, we use the procedure that calculates the coherence spectrum between the LOD time series and the first principal component.

The time-frequency diagram in Fig. 5 illustrates the evolution of the quadratic coherence spectrum between two time series shown in Fig. 3. Estimation was carried out in a moving time window with a length of 182 days shifted by 5 days using a 2D vector autoregression model of order 5 (Marple, 1987) with preliminary linear detrending and passing to increments. This approach has been already used in (Lyubushin, 2020a; 2020b) for analyzing the trends in the properties of global seismic noise and their relation with nonuniform rotation of the Earth. From Fig. 5 it can be seen that the bursts in coherence are localized within a narrow frequency band with periods from 11 to 14 days.

Figure 6 shows the graphs of the coherence bursts maxima in each time window for periods from 11 to 14 days and the graph of the logarithm of energy (J) released due to the seismic events in the Kamchatka region, also in a 182-day moving time window with a shift of 5 days.

In Fig. 6 it can be visually noticed that the curve of the logarithm of released energy is frequently delayed relative to the curve of the coherence spectrum max-

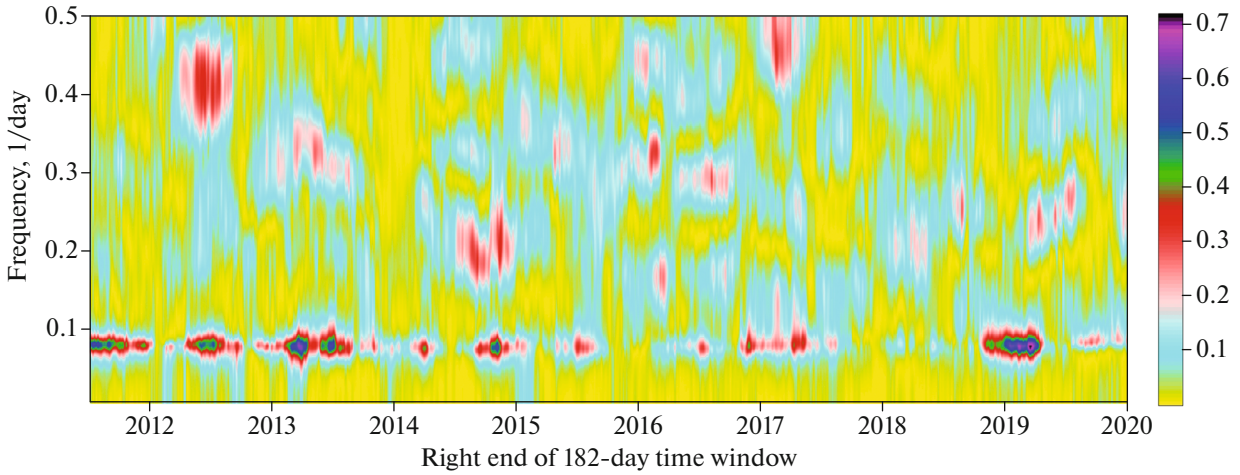

Fig. 5. Frequency-time diagram of quadratic spectrum of coherence between LOD and first principal component of three characteristics of seismic noise in 182-day moving window shifted by 5 days.

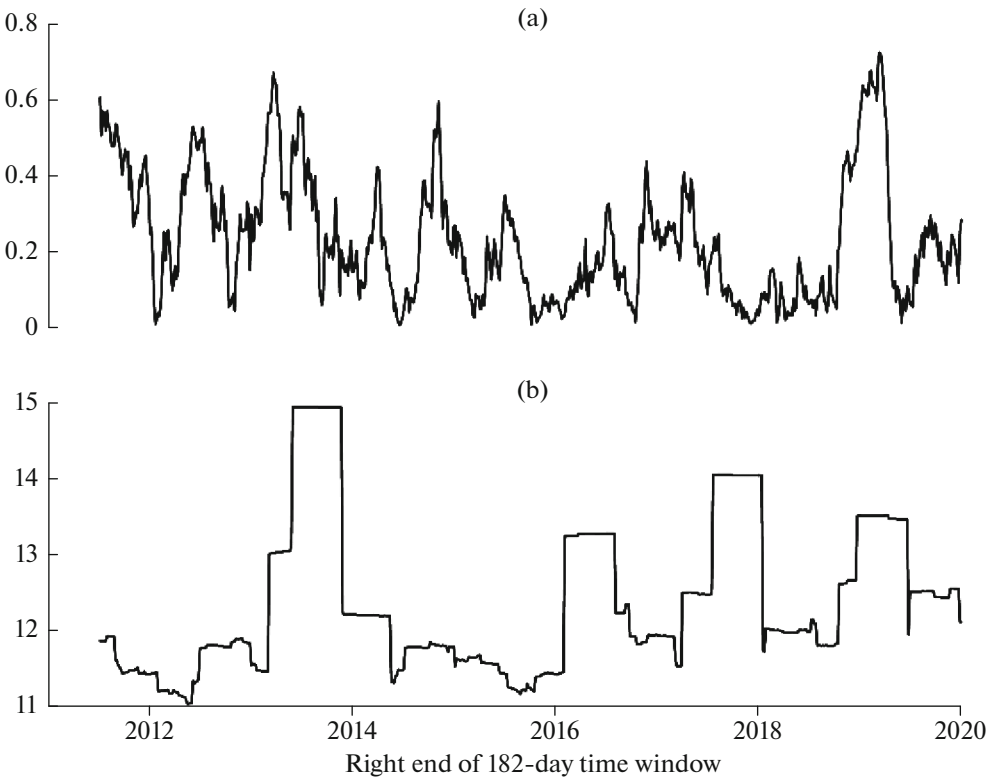

Fig. 6. (a) Maximum squared coherence between LOD and first principal component of three daily characteristic of seismic noise; (b) common logarithm of energy (J) released in seismic events in rectangular region 50°–60° N, 153°–170° E (https://www.usgs.gov/; http://glob.emsd.ru/).

ima estimated in a 182-day moving time window with a shift of 5 days. Let us quantify this delay by calculating the cross-correlation function whose graph is shown in Fig. 7.

In Fig. 7, the values of the cross-correlation function are taken with a lag from –250 to 250 days (±50 points with a time step of 5 days). The maximum of the correlation coefficient between the maximum coherence of LOD variations and seismic noise falls on 95 days (19 time shifts), indicating that, on average, the effect of the increase of their coherence leads the release of seismic energy in the Kamchatka region.

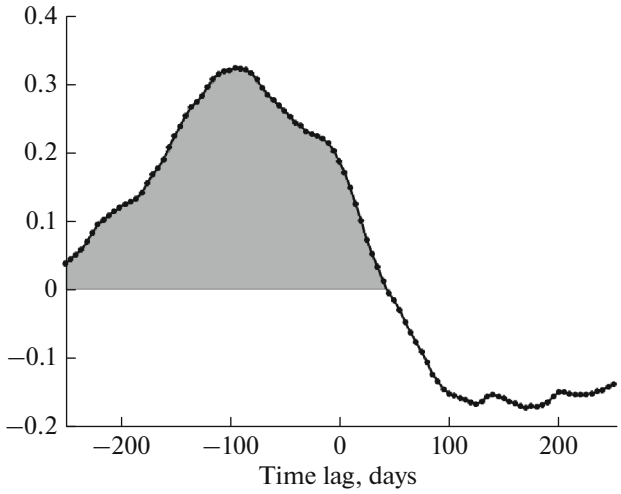

Fig. 7. Correlation coefficients between log energy release in seismic events in Kamchatka region in 182-day moving window shifted by 5 days and maximum value of quadratic coherence spectrum between LOD and first principal component of three daily median characteristics of seismic noise.

The graphs in Fig. 6 show that the time shift between the compared curves is not constant but varies. We complement the mean estimate of cross-correlation presented in Fig. 7 with a similar estimate in a moving time window. It should be noted that in our estimates, one (182-day long) time window is already present. Let us call it a short one. Now, we intend to obtain cross-correlation estimates in a "long" time window which is composed of a number of "short" windows. The length of the "long" window should be selected with the allowance for the fact that the coherences were obtained by estimating in the "short" time windows with a length of 182 days that were shifted by 5 days. Thus, if we take L adjacent coherence values, then the dimensional length of the "long" time window will be $N = 182 + (L-1)\times 5$ days. Choosing $L = 330$, we obtain $N = 1827$ days. The number of days in five adjacent years is 1826 or 1827, given that in each 5-year interval, one or two years are leap years. Therefore, the choice of $L = 330$ highly accurately provides a time window with a length of 5 years.

The graph in Fig. 8a shows the behavior of the maximum value of the correlation coefficient between the coherences and the logarithms of the released energy in a moving time window with a length of 330 adjacent points (about 5 years) with a minimum shift by one point (5 days). The maxima are taken over the mutual time lags by ±50 points within the "large" window with a time step of 5 days.

The estimate of the time lag that provides cross-correlation maximum (in modulus) is shown in the

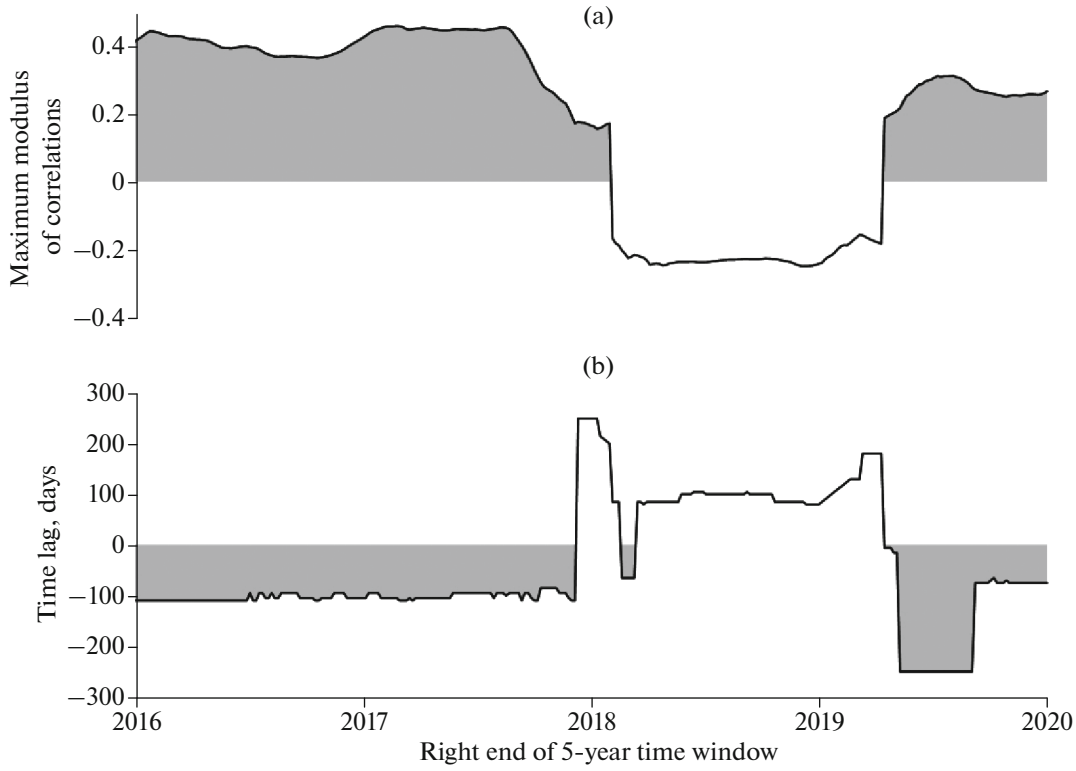

Fig. 8. (a) Graph of maximum modulus of correlation coefficient between coherences and logarithms of released energy in 5-year window with lags from −250 to 250 days; (b) graph of lag (in days) within 5-year time window providing maximum modulus of correlation coefficient. Negative lags corresponding to lead of seismic energy release relative to bursts in coherence are shaded.

graph in Fig. 8b. It can be seen here that during most of the considered interval, the time lag is negative which corresponds to the lead of the release of seismic energy with respect to the bursts in coherence. We noted that the median value of the optimal time lags Fig. 8b is 95 days, i.e., exactly the value providing the average cross-correlation maximum in Fig. 7.

CONCLUSIONS

The method for studying the time-frequency relationship between a set of median characteristics of seismic noise recorded by seismic networks in a given region and the time series of the length of day characterizing the nonuniform rotation of the Earth has been developed. Application of the method for processing continuous seismic noise data recorded in 2011–2019 by the network stations in Kamchatka provided a time series of the bursts of coherence estimated in a half-year moving time window. The cross-correlation analysis of the variations in the coherence maxima and the logarithm of energy release by seismic events in Kamchatka in the time window of the same length revealed a predominant delay of the intensity of the seismic process relative to the variations in coherence. This fact is interpreted as a manifestation of the triggering effect of the nonuniform rotation of the Earth on the seismic process.

FUNDING

The work was supported by the Russian Foundation for Basic Research under project no. 18-05-00133.

REFERENCES

Aivazyan, S.A., Bukhshtaber, V.M., Enyukov, I.S., and Meshalkin, L.D., *Prikladnaya statistika. Klassifikatsiya i snizhenie razmernosti* (Applied Statistics. Classification and Dimensionality Reduction), Aivazyan, S.A., Ed., Moscow: Finansy i statistika, 1989.

Bendick, R. and Bilham, R., Do weak global stresses synchronize earthquakes?, *Geophys. Res. Lett.*, 2017, vol. 44, pp. 8320–8327.
https://doi.org/10.1002/2017GL074934

Chebrov, V.N., Regional seismic monitoring system, *Tr. 4 nauchno-tekhn. konf.: Problemy kompleksnogo geofizicheskogo monitoringa Dal'nego Vostoka Rossii* (Proc. 4th Sci. Tech. Conf.: Problems of Complex Geophysical Monitoring of the Russian Far East), Petropavlovsk-Kamchatskii, 2013, Obninsk: GS RAN, 2013, pp. 8–15.

Chebrov, V.N., Droznin, D.V., Kugaenko, Yu.A., Levina, V.I., Senyukov, S.L., Sergeev, V.A., Shevchenko, Yu.V., and Yashchuk, V.V., The system of detailed seismological observations in Kamchatka in 2011, *J. Volcanol. Seismol.*, 2013, vol. 7, no. 1, pp. 16–36.

Feder, J., *Fractals*, New York: Plenum Press, 1988.

Guberman, Sh.A., D-waves, and nonuniformity of the Earth rotation, *Dokl. Akad. Nauk SSSR*, 1976, vol. 230, no. 4, pp. 811–814.

Jolliffe, I.T., *Principal Component Analysis*, New York: Springer, 1986.
https://doi.org/10.1007/b98835

Kasimova, V.A., Kopylova, G.N., and Lyubushin, A.A., Variations in the parameters of background seismic noise during the preparation stages of strong earthquakes in the Kamchatka region, *Izv. Phys. Solid Earth*, 2018, vol. 54, no. 2, pp. 269–283.

Levin, B.W., Sasorova, E.V., Steblov, G.M., Domanski, A.V., Prytkov, A.S., and Tsyba, E.N., Variations of the Earth's rotation rate and cyclic processes in geodynamics, *Geod. Geodyn.*, 2017, no. 8, pp. 206–212.
https://doi.org/10.1016/j.geog.2017.03.007

Levitskii, L.S., Rykhlova, L.V., and Sidorenkov, N.S., El Niño southern oscillation and Earth rotation irregularity, *Astron. Zh.*, 1995, vol. 72, no. 2, pp. 272–276.

Lyubushin, A.A., *Analiz dannykh sistem geofizicheskogo i ekologicheskogo monitoringa* (Data Analysis of Geophysical and Environmental Monitoring Systems), Moscow: Nauka, 2007.

Lyubushin, A.A., Synchronization trends and rhythms of multifractal parameters of the field of low-frequency microseisms, *Izv. Phys. Solid Earth*, 2009, vol. 45, no. 5, pp. 381–394.

Lyubushin, A.A., Multifractal parameters of low-frequency microseisms, Ch. 15 of *Synchronization and Triggering: from Fracture to Earthquake Processes*, de Rubeis, V., Czechowski, Z., and Teisseyre, R., Eds., GeoPlanet: Earth and Planet. Sci. Ser., vol. 1, Berlin: Springer, 2010, pp. 253–272.
https://doi.org/10.1007/978-3-642-12300-9_15

Lyubushin, A.A., Prognostic properties of low-frequency seismic noise, *Nat. Sci.*, 2012, vol. 4, pp. 659–666.
https://doi.org/10.4236/ns.2012.428087

Lyubushin, A.A., How soon would the next mega-earthquake occur in Japan?, *Nat. Sci.*, 2013, no. 5, pp. 1–7.
https://doi.org/10.4236/ns.2013.58A1001

Lyubushin, A.A., Analysis of coherence in global seismic noise for 1997–2012, *Izv. Phys. Solid Earth*, 2014a, vol. 50, no. 3, pp. 325–333.

Lyubushin, A.A., Dynamic estimate of seismic danger based on multifractal properties of low-frequency seismic noise, *Nat. Hazards*, 2014b, vol. 70, pp. 471–483.
https://doi.org/10.1007/s11069-013-0823-7

Lyubushin, A., Synchronization of geophysical fields fluctuations, Ch. 6 of *Complexity of Seismic Time Series: Measurement and Applications*, Chelidze, T., Telesca, L., and Vallianatos, F., Eds., Amsterdam: Elsevier, 2018, pp. 161–197.
https://doi.org/10.1016/B978-0-12-813138-1.00006-7

Lyubushin, A., Connection of seismic noise properties in Japan and California with irregularity of Earth's rotation, *Pure Appl. Geophys.*, 2020a, vol. 177, pp. 4677–4689.
https://doi.org/10.1007/s00024-020-02526-9

Lyubushin, A.A., Seismic noise wavelet-based entropy in Southern California, *J. Seismol.*, 2020b.
https://doi.org/10.1007/s10950-020-09950-3

Lyubushin, A.A., Trends of global seismic noise properties in connection to irregularity of Earth's rotation, *Pure Appl. Geophys.*, 2020c, vol. 177, no. 2. pp. 621–636.
https://doi.org/10.1007/s00024-019-02331-z

Lyubushin, A.A., Kopylova, G.N., Kasimova, V.A., and Taranova, L.N., The properties of fields of low frequency noise from the network of broadband seismic stations in Ka-

mchatka, *Vestn. KRAUNTs, Nauki Zemle*, 2015, no. 2 (26), pp. 20–36. http://www.kscnet.ru/kraesc/2015/2015_26/art3.pdf.

Mallat, S.A., *Wavelet Tour of Signal Processing*, 2nd ed., San Diego: Academic Press, 1999.

Marple, S.L., Jr., *Digital Spectral Analysis with Applications*, Englewood Cliffs: Prentice-Hall, 1987.

Milyukov, V.K., Vinogradov, M.P., Mironov, A.P., Myasnikov, A.V., and Perelygin, N.A., The free oscillations of the Earth excited by three strongest earthquakes of the past decade according to deformation observations, *Izv. Phys. Solid Earth*, 2015, vol. 51, no. 2, pp. 176–190.

Sasorova, E.V. and Levin, B.W., On the connection of variations of the velocity of the Earth rotation and its seismic activity. The Earth's entry into a new phase of reducing of the angular velocity rotation, *Vestn. KRAUNTs, Fiz.-mat. nauki*, 2017, no. 4(20), pp. 91–100.
https://doi.org/10.18454/2079-6641-2017-20-4-91-100

Shanker, D., Kapur, N., and Singh, V., On the spatio temporal distribution of global seismicity and rotation of the Earth – A review, *Acta Geod. Geophys. Hung.*, 2001, vol. 36, pp. 175–187.
https://doi.org/10.1556/AGeod.36.2001.2.5

Sidorenkov, N.S., *Atmosfernye protsessy i vrashchenie Zemli* (Atmospheric Processes and the Rotation of the Earth), St. Petersburg: Gidrometeoizdat, 2002.

Sobolev, G.A., *Seismicheskii shum* (Seismic Noise), Moscow: Nauka obraz., 2014.

Zotov, L., Sidorenkov, N.S., Bizouard, C., Shum, C.K., and Shen, W., Multichannel singular spectrum analysis of the axial atmospheric angular momentum, *Geod. Geodyn.*, 2017, vol. 8, no. 6, pp. 433–442.
https://doi.org/10.1016/j.geog.2017.02.010

Translated by M. Nazarenko